

# Fractional (Cauchy) and quasirelativistic spectral problems

Piotr Garbaczewski (Opole, Poland)

About:  $H = T + V,$   $T_m = \sqrt{-\hbar^2 c^2 \Delta + m^2 c^4} - mc^2$   $T_0 = \hbar c |\nabla|$

Confining  $V=V(x)$ : **harmonic** or **finite well** of arbitrary depth

- **Lévy-Schrödinger semigroups** - additive perturbations of nonlocal noise generators, spectral properties
- **Pseudo-differential QM** - analytic continuation in time, holomorphic semigroups, unitary dynamics, spectral problems, nonlocally induced (ground-state) jump-type processes
- **Math:** „spectral properties of the Cauchy or quasirelativistic process” (Kaleta, Kulczycki, Kwaśnicki, Malecki, Stós, Lörinczi)
- **Phys:** „Schrödinger-type eigenvalue problems for  $H= T + V$ ” (P.G.)

*Lost in **math-phys** translation:*

- graph, wedge, vertex **vs** network/lattice, link, node)
- Stochastic process in the interval **vs** random motion in the infinite well
- Fractional Laplacian in the interval **vs** Fractional spectral problem in the infinite well

## Uses of Lévy-Schrödinger semigroup kernels

$\hat{H} = -\Delta + V \geq 0$  the integral kernel of  $\exp(-t\hat{H})$  reads  $k(y, x, t) = k(x, y, t) = \sum_j \exp(-\epsilon_j t) \Phi_j(y) \Phi_j^*(x)$ .

### First input: Schrödinger's boundary data problem (1932)

Deduce the Markovian interpolation consistent with a given pair of boundary measure data at fixed initial and terminal time instants  $t_1 < t_2$ ;  $A$  and  $B$  are two Borel sets in  $R$ .

$$m(A, B) = \int_A dx \int_B dy m(x, y),$$

$$\int_R m(x, y) dy = \rho(x, t_1),$$

$$\int_R m(x, y) dx = \rho(y, t_2),$$

where

$$m(x, y) = f(x)k(x, t_1, y, t_2)g(y)$$

$f(x)$  and  $g(y)$  are of the same sign and nonzero,  $k(x, s, y, t)$  is an a priori chosen, bounded strictly positive and continuous (dynamical semigroup) kernel,  $t_1 \leq s < t \leq t_2$ .

Prescribing  $k(x, s, y, t)$  in advance, we have functions  $f(x), g(y)$  determined uniquely (up to constant factors) by marginal data, c.f. Beurling, Fortet, Jamison.

By denoting

$$\theta_*(x, t) = \int f(z)k(t_1, z, x, t)dz$$

$$\theta(x, t) = \int k(x, t, z, t_2)g(z)dz$$

it follows that

$$\rho(x, t) = \theta(x, t)\theta_*(x, t) = \int p(y, s, x, t)\rho(y, s)dy,$$

$$p(y, s, x, t) = k(y, s, x, t)\frac{\theta(x, t)}{\theta(y, s)},$$

$$t_1 \leq s < t \leq t_2$$

**Note:** If we assume that  $g(x) = \rho_*^{1/2}(x)$ , then likewise  $\theta(x) = \rho_*^{1/2}(x)$ , so we end up with previously mentioned Doob's type mapping of a semigroup kernel into a transition density.

Useful (derived) concept:

**Targeted stochasticity:** given a predefined **pdf**; can it be interpreted as a unique **asymptotic invariant** pdf of a certain (Markovian ?) stochastic process.

**Hint:** the ground state (square root of the pdf) of the confining semigroup does the job; see the boxed text in the above.

## Second input: elementary harmonic/functional analysis

Let us consider self-adjoint operators (Hamiltonians) with dense domains in  $L^2(R)$ , of the form  $\hat{H} = F(\hat{p})$ , where  $\hat{p} = -i\nabla$  and for  $-\infty < k < +\infty$ ,  $F = F(k)$  is a real valued, bounded from below, locally integrable function. For  $t \geq 0$  we have:

$$\exp(-t\hat{H}) = \int_{-\infty}^{+\infty} \exp[-tF(k)]dE(k)$$

$dE(k)$  is the spectral measure of  $\hat{p}$ .

Let us set

$$k_t = \frac{1}{\sqrt{2\pi}}[\exp(-tF(p))]^\vee$$

then the action of  $\exp(-t\hat{H})$  can be given in terms of a convolution:  $\exp(-t\hat{H})f = f * k_t$ , where  $(f * g)(x) := \int_R g(x - z)f(z)dz$ .

If  $F(p)$  satisfies the Lévy-Khintchine formula, then  $k_t$  is a positive measure for all  $t \geq 0$  and we arrive at the simplest (free noise) positivity preserving semigroups.

The integral part of the L-K formula is responsible for random jumps ( $\nu(dy)$  stands for the Lévy measure):

$$F(p) = - \int_{-\infty}^{+\infty} [\exp(ipy) - 1 - \frac{ipy}{1 + y^2}] \nu(dy)$$

### Third input: (pseudo) relativistic Hamiltonians

R. Carmona, (1988)

$$F_0(p) = |p|$$

$$F_m(p) = \sqrt{p^2 + m^2} - m, \quad m > 0$$

(better known as  $H_{cl} = \sqrt{m^2 c^4 + c^2 p^2} - mc^2$ )

Within the ramifications of the Schrödinger boundary data problem set  $\theta(x, t) \equiv 1$  and  $\theta_*(x, t) \doteq \rho(x, t)$  so that

$$[\exp(-t\hat{H})\rho](x) = \rho(x, t)$$

where  $F(p \rightarrow -i\nabla) := \hat{H}$  implies

$$F_0(p) \implies \partial_t \rho(x, t) = -|\nabla| \rho(x, t)$$

$$F_m(p) \implies \partial_t \rho(x, t) = -[\sqrt{-\Delta + m^2} - m] \rho(x, t)$$

$F_0$  is a special (Cauchy) case of the symmetric stable probability laws and readily generalizes to (we can parallel this step by a lift from  $R$  to  $R^n$ )

$$F_\mu = |p|^\mu \rightarrow \partial_t \rho(x, t) = -|\Delta|^{\mu/2} \rho(x, t)$$

with  $0 < \mu < 2$ . (Note:  $\partial_t \rho = \Delta \rho$  derives from the Wiener process and  $\hat{H} = -\Delta$ )

# „Rough” conceptual guide: 1D Cauchy semigroup

P. Garbaczewski, R. Olkiewicz, J. Math. Phys. **40**, 1057, (1999)

$$\partial_t \theta_* = -|\nabla| \theta_* - V \theta_*, \quad \partial_t \theta = |\nabla| \theta + V \theta, \quad (21)$$

where  $V$  is a measurable function such that:

- (a) for all  $x \in R$ ,  $V(x) \geq 0$ ,
- (b) for each compact set  $K \subset R$  there exists  $C_K$  such that for all  $x \in K$ ,  $V$  is locally bounded  $V(x) \leq C_K$ .

*Lemma 5:* If  $1 \leq r \leq p \leq \infty$  and  $t > 0$ , then the operators  $T_t^V$  defined by

$$(T_t^V f)(x) = E_x^C \left\{ f(X_t^C) \exp \left[ - \int_0^t V(X_s^C) ds \right] \right\}$$

are bounded from  $L^r(R)$  into  $L^p(R)$ . Moreover, for each  $r \in [1, \infty]$  and  $f \in L^r(R)$ ,  $T_t^V f$  is a bounded and continuous function.

*Lemma 7:* For any  $p \in [1, \infty]$  and  $f \in L^p(R)$  there holds

$$(T_t^V f)(x) = \int_R k_t^V(x, y) f(y) dy, \quad \text{where } k_t^V(x, y) \geq 0 \text{ almost everywhere}$$

*Lemma 8:*  $k_t^V(x,y)$  is jointly continuous in  $(x,y)$ .

*Lemma 9:*  $k_t^V(x,y)$  is strictly positive.

let  $\rho_0(x)$  and  $\rho_T(x)$  be strictly

positive densities. Then, the Markov process  $X_t^V$  characterized by the transition probability density:

$$p^V(y,s,x,t) = k_{t-s}^V(x,y) \frac{\theta(x,t)}{\theta(y,s)} \quad (23)$$

and the density of distributions

$$\rho(x,t) = \theta_*(x,t)\theta(x,t),$$

where

$$\theta_*(x,t) = \int_R k_t^V(x,y)f(y)dy, \quad \theta_*(y,t) = \int_R k_{T-t}^V(x,y)g(x)dx$$

is precisely that interpolating Markov process to which Theorem 1 extends its validity, when the perturbed semigroup kernel replaces the Cauchy kernel.

Clearly, for all  $0 \leq s \leq t \leq T$  we have

$$\theta_*(x,t) = \int_R k_{t-s}^V(x,y)\theta_*(y,s)dy, \quad \theta(y,s) = \int_R k_{t-s}^V(x,y)\theta(x,t)dx \quad (24)$$

Association: set  $\theta_* = \Psi$ ,  $\theta = \rho_*^{1/2}$ , so getting  $\rho(x,t) = (\theta\theta_*)(x,t) = \Psi(x,t)\rho_*^{1/2}(x)$  and  $\partial_t \Psi = -\hat{H}\Psi$  with  $\hat{H} = |\nabla| + V$

# Appetizer: ground state of the Cauchy oscillator

Physica A (2010)

$$\hat{H}_{1/2} \equiv \lambda |\nabla| + \left( \frac{\kappa}{2} x^2 - \mathcal{V}_0 \right)$$

$$\hat{H} = -D\Delta + \left( \frac{\gamma^2 x^2}{4D} - \frac{\gamma}{2} \right)$$

direct reconstruction route:

$$\left( \frac{\kappa}{2} x^2 - \mathcal{V}_0 \right) \rho_*^{1/2} = -\lambda |\nabla| \rho_*^{1/2}$$

$\tilde{f}(p)$  the Fourier transform of  $f = \rho_*^{1/2}(x)$

$$-\frac{\kappa}{2} \Delta_p \tilde{f} + \gamma |p| \tilde{f} = \mathcal{V}_0 \tilde{f}$$

$$k = (p - \sigma)/\zeta$$

$$\psi(k) = \tilde{f}(p) \quad \sigma = \mathcal{V}_0/\gamma$$

$$\zeta = (\kappa/2\gamma)^{1/3}$$

$$\frac{d^2 \psi(k)}{dk^2} = |k| \psi(k)$$



A unique normalized ground state function

of

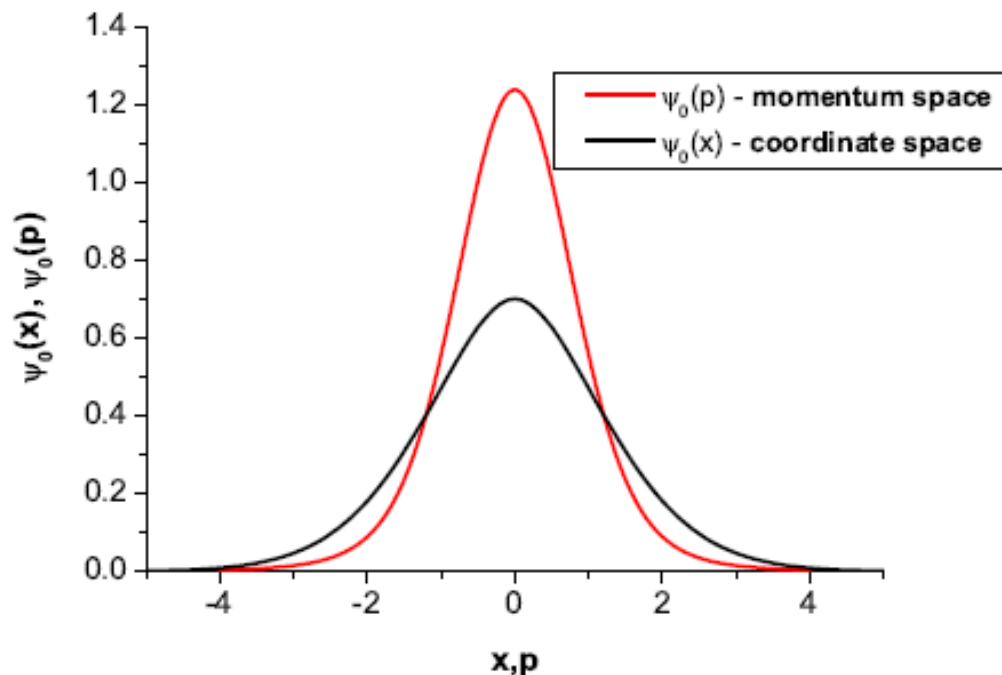
$$\frac{d^2\psi(k)}{dk^2} = |k|\psi(k)$$

is composed of two Airy pieces

that are glued together at the first zero  $y_0$  of the Airy function derivative:

$$\psi_0(k) = A_0 \begin{cases} \text{Ai}(-y_0 + k), & k > 0 \\ \text{Ai}(-y_0 - k), & k < 0, \end{cases}$$

$$A_0 = [\text{Ai}(-y_0)\sqrt{2y_0}]^{-1}, \quad y_0 \approx 1.01879297$$



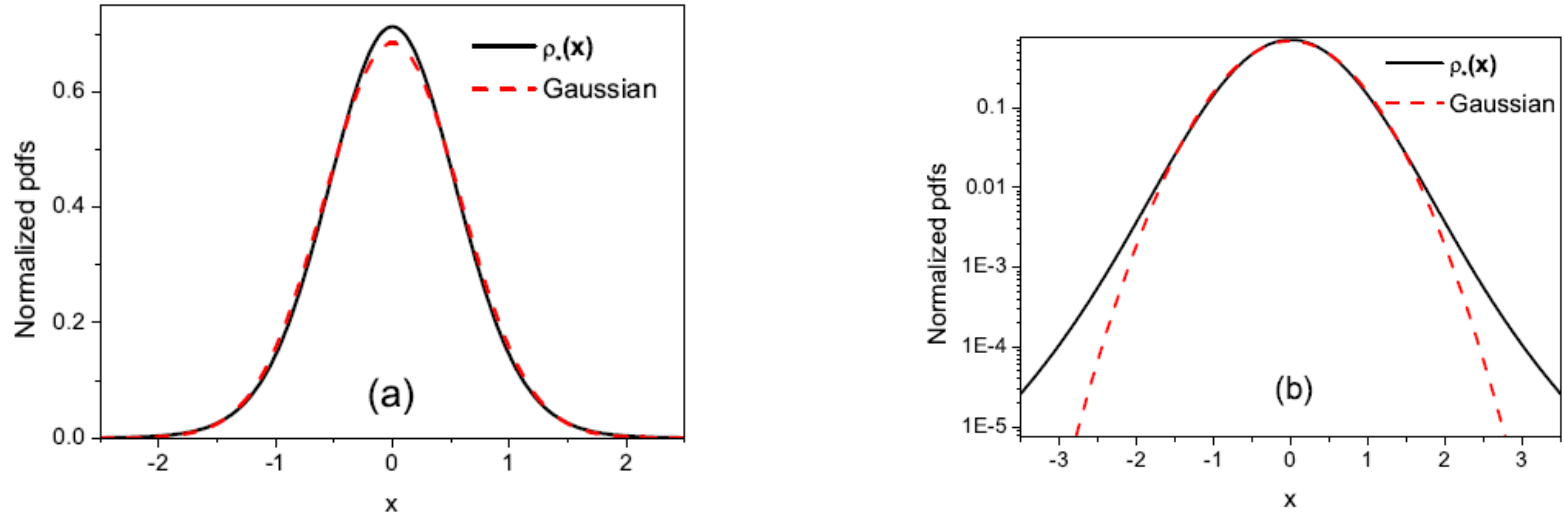


FIG. 7: Normalized invariant pdf (30) (full line) for the quadratic semigroup potential. The Gaussian function, centered at  $x = 0$  and with the same variance  $\sigma^2 = 0.339598$  is shown for comparison. Panel (a) shows functions in linear scale, while panel (b) shows them in logarithmic scale to better visualize their different behavior.

$$\psi_0(x) = \frac{A_0}{\pi} \int_{-y_0}^{\infty} \text{Ai}(t) \cos x(t + y_0) dt = \rho_*^{1/2}(x)$$

K. Kaleta and T. Kulczycki (2009) - **asymptotic decay of eigenfunctions**

$\psi_0$  for  $\hat{H}_\mu = |\Delta|^\mu + (x^2 - \mathcal{V}_0)$  displays  $\sim |x|^{-(3+\mu)}$  heavy tail for  $|x| \gg 1$

## Some (minor ?) **quiries/problems** (Bielefeld, July 2012)

**Lévy-Schrödinger semigroups** – the induced pdf dynamics needs further exploration, no rigorous results about  $X(t)$  (except for the 1D Cauchy driver, JMP **40**, 1057, (1999)), sample path properties basically unknown (computer-assisted work in progress), Markovianess not necessarily obvious, albeit seemingly valid

**Pseudo-differential spectral problems** are hard or intractable, only a limited number of solvable cases (stability of matter issues are well developed, c.f. E. Lieb et al., not mentioned here). Scarce analytic access to ground states and other eigenfunctions, not even mentioning the eigenvalues.

Current status, as for 30 May 2014

### **Spectral properties- what do we know ?**

**Phys:** a number of plainly wrong results on eigenvalues and shapes of eigenfunctions in the **physics** oriented literature, no explicit insight into elementary confining spectral problems.

**Math:** rigorous estimates and approximate spectral solutions for the infinite well (Cauchy and quasirelativistic) and Cauchy oscillator.

**Today topics:** quasirelativistic oscillator and finite well ( $m>0$ );  $m=0$  spectral solutions as the reference and the validity control.

## Solving Schrödinger-type spectral problems: **Cauchy oscillator** and **finite well**

$$T \psi(x) = (-\Delta)^{1/2} \psi(x) = \frac{1}{\pi} \int \frac{\psi(x) - \psi(x+z)}{z^2} dz$$

$$H = T + V$$

$$H \psi_i(x) = E_i \psi_i(x), \quad i = 1, 2, \dots,$$

Computer assisted approach: **spectrum-generating algorithm**

$$e^{-hH} \approx e^{-\frac{h}{2}V} (1 - hT) e^{-\frac{h}{2}V} \doteq \mathcal{S}(h).$$

$$\psi(x, t) = [e^{-tH} \psi](x, 0) \quad \Delta t \doteq h \quad \psi(x, 0) \rightarrow \psi(x, kh)$$

$$k = 1, 2, \dots,$$

(i) We choose a finite number  $n$  of trial state vectors (preferably linearly independent)  $\{\Phi_i^{(0)}, 1 \leq i \leq n\}$ , where  $n$  is correlated with an ultimate number of eigenvectors of  $H$  to be obtained in the numerical procedure; at the moment we disregard an issue of their optimal (purpose-dependent) choice.

(ii) For all trial functions the time evolution beginning at  $t = 0$  and terminating at  $t = h$ , for all  $1 \leq i \leq n$  is mimicked by the time shift operator  $S(h)$  of Eq. (5)

$$\Psi_i^{(1)}(x) = S(h)\Phi_i^{(0)}(x). \quad (6)$$

(iii) The obtained set of linearly independent vectors  $\{\Psi_i^{(1)}\}$  should be made orthogonal (we shall use the familiar Gram-Schmidt procedure, although there are many others, [7]) and normalized. The outcome constitutes a *new* set of trial states  $\{\Phi_i^{(1)}, i = 1, 2, \dots, n\}$ .

(iv) Steps (ii) and (iii) are next repeated consecutively, giving rise to a temporally ordered sequence of  $n$ -element orthonormal sets  $\{\Phi_i^{(k)}(x), i = 1, 2, \dots, n\}$  and the resultant set of linearly independent vectors

$$\Psi_i^{(k+1)}(x) = S(h)\Phi_i^{(k)}(x), \quad i = 1, 2, \dots, n,$$

at time  $t_{k+1} = (k + 1) \cdot h$ .

(v) The temporally ordered sequence of  $\Phi_i^{(k)}(x)$ ,  $k \geq 1$  for sufficiently large  $k$  is expected to converge to an eigenvector of  $S(h)$ , according to:

$$S(h)\Phi_i^{(k)}(x) = e^{-hE_i^{(k)}}\Phi_i^{(k)}(x) \approx e^{-hE_i}\psi_i(x), \quad (7)$$

where  $\psi_i$  actually stands for an eigenvector of  $H$  corresponding to the eigenvalue  $E_i$ . Here:

$$E_i^{(k)}(h) = -\frac{1}{h} \ln(\mathcal{E}_i^k(h)), \quad (8)$$

where

$$\mathcal{E}_i^k(h) = \langle \Phi_i^{(k)} | \Psi_i^{(k+1)} \rangle = \langle \Phi_i^{(k)} | S(h)\Phi_i^{(k)} \rangle,$$

is an expectation value of  $S(h)$  in the  $i$ -th state  $\Phi_i^{(k)}$ .

It is the evaluation of  $\Phi_i^{(k)}(x)$  and  $E_i^{(k)}(h)$  that is amenable to computing routines and yields approximate eigenfunctions and eigenvalues of  $H$ . The degree of approximation accuracy is set by the terminal time value  $t_k = kh$ , at which earlier detected symptoms of convergence ultimately stabilize, so that the iteration (i)-(v) can be stopped.

## Cauchy oscillator test.

In  $1D$ , from the start we need to choose  $x \in [-a, a]$ ,  $a > 0$

In view of the a priori declared  $[-a, a]$  integration boundary limits, irrespective of the initial data choice  $\{\Phi_i^{(0)} \in L^2(\mathbb{R})\}$ , the simulation outcome is automatically placed in  $L^2([-a, a])$ .

For the Cauchy oscillator whose eigenfunctions extend over the whole real line, we effectively get an approximation of true eigenfunctions by functions with a support restricted to  $[-a, a]$ . Clearly, the value of  $a$  cannot be too small and for the present purpose the minimal value of  $a = 50$  has been found to be a reliable choice. This point must be continually kept in mind.

For our purposes the natural  $L^2(\mathbb{R})$  choice of initially given trial state vectors is that of Hermite functions

$$\Phi_{i+1}^{(0)}(x) = \frac{1}{\sqrt{2^i i!} \sqrt{\pi}} H_i(x) e^{-x^2/2}, \quad i = 0, 1, \dots \quad (9)$$

where  $H_i(x)$  are Hermite polynomials, defined by the Rodrigues formula

$$H_i(x) = (-1)^i e^{x^2} \frac{d^i}{dx^i} e^{-x^2}, \quad i = 0, 1, \dots$$

We recall that  $H_0(x) = 1$ ,  $H_1(x) = 2x$ ,  $H_2(x) = 4x^2 - 2$ ,  $H_3(x) = 8x^3 - 12x$  and so on.

The functions (9) form a standard (quantum harmonic oscillator) basis in  $L^2(\mathbb{R})$ . They loose this property after the first time-shift operation (6), being mapped into linearly independent functions with support restricted to  $[-a, a]$ .

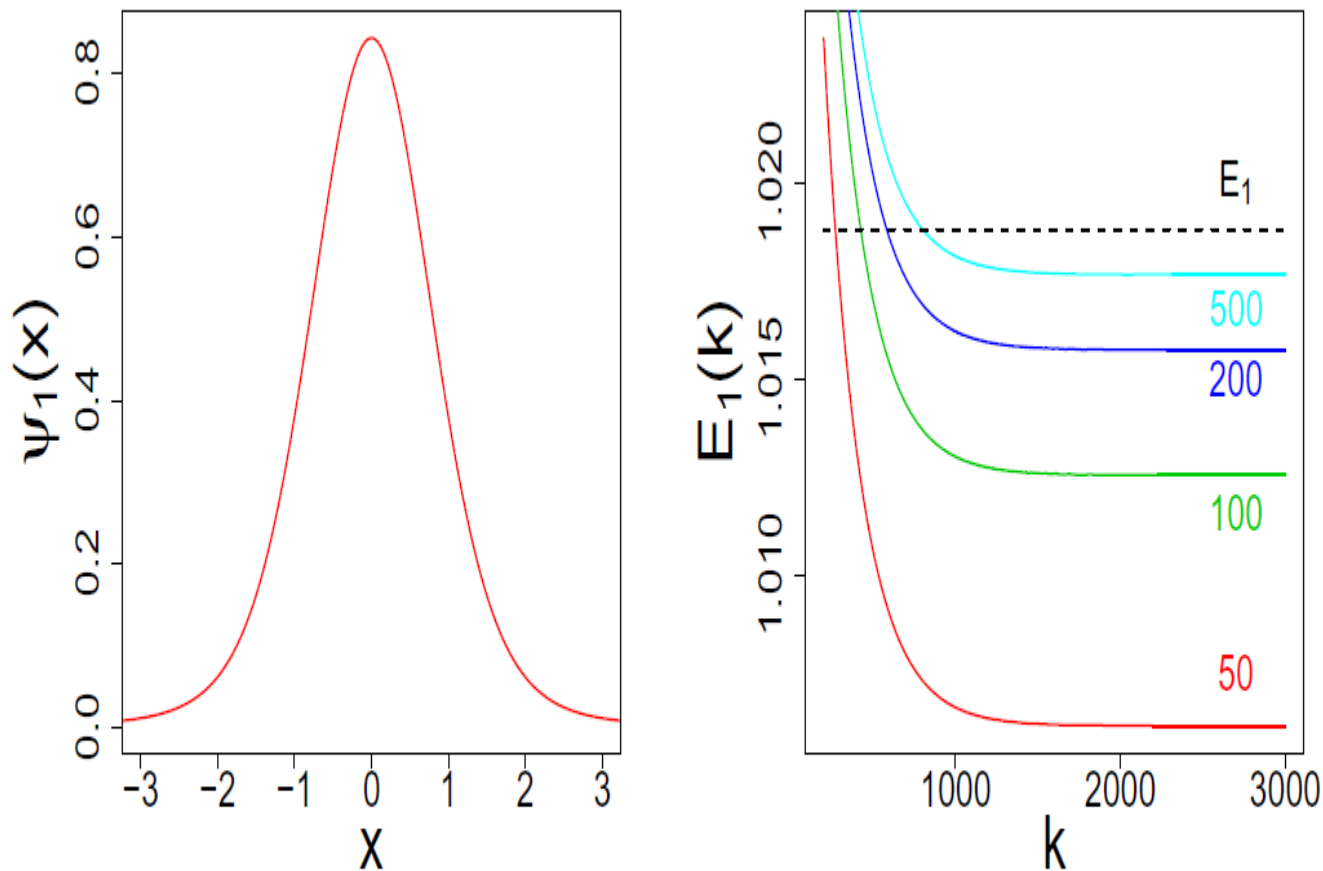


FIG. 1: Cauchy oscillator ground state (left panel) and the  $(k)$ -time evolution of  $E_1^{(k)}(h) = -\frac{1}{h} \ln(\mathcal{E}_1^k(h))$ , (8), for  $a = 50, 100, 200, 500$ . The dotted line indicates the ground state eigenvalue reported in Refs. [24, 25].



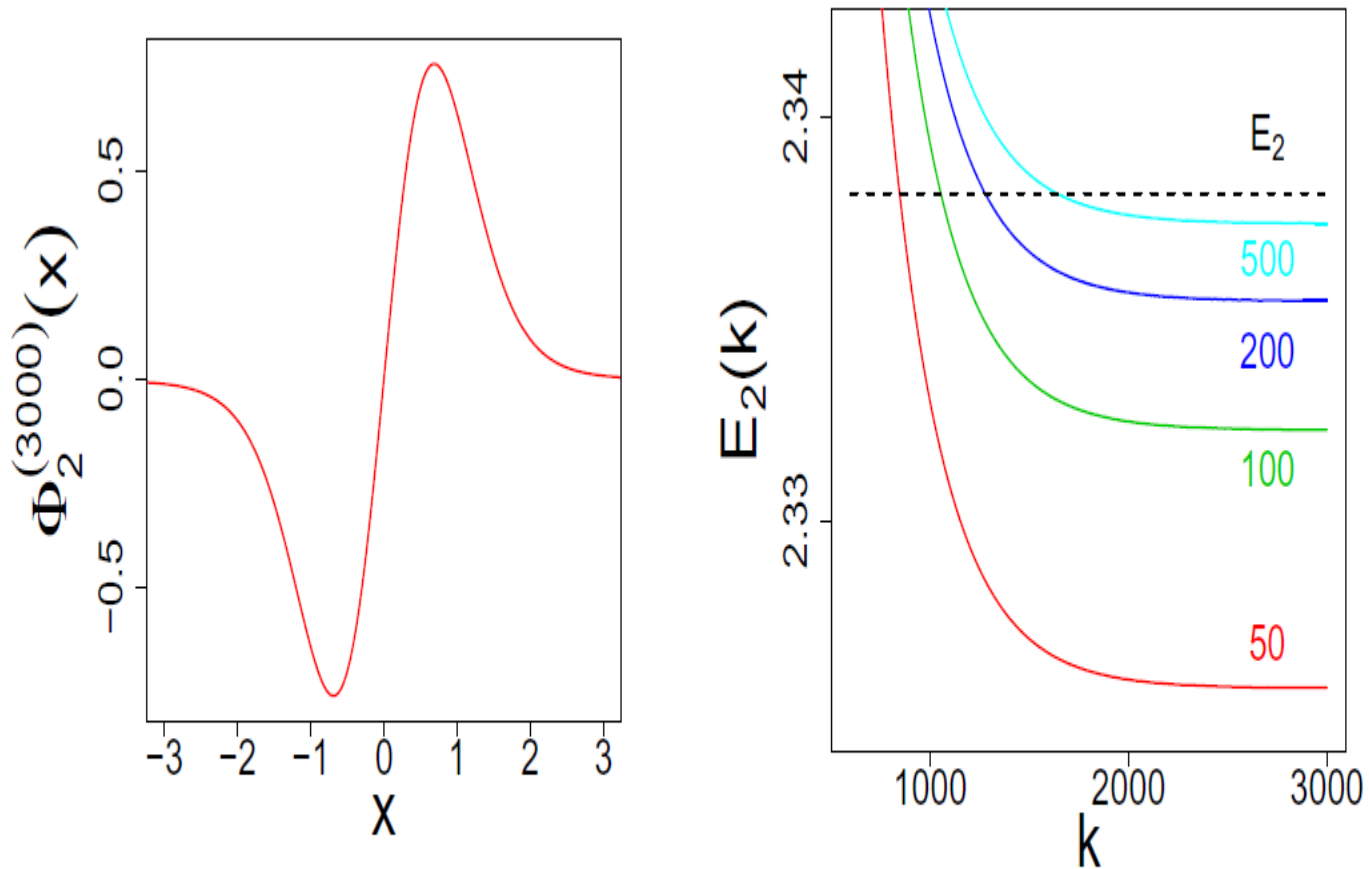


FIG. 3: First excited state  $\psi_2$  of the Cauchy oscillator and the  $(k)$ -time evolution of  $E_2^{(k)}(h)$  (8) for  $a = 50, 100, 200, 500$ . The dotted line indicates the first excited eigenvalue reported in Refs. [24, 25].

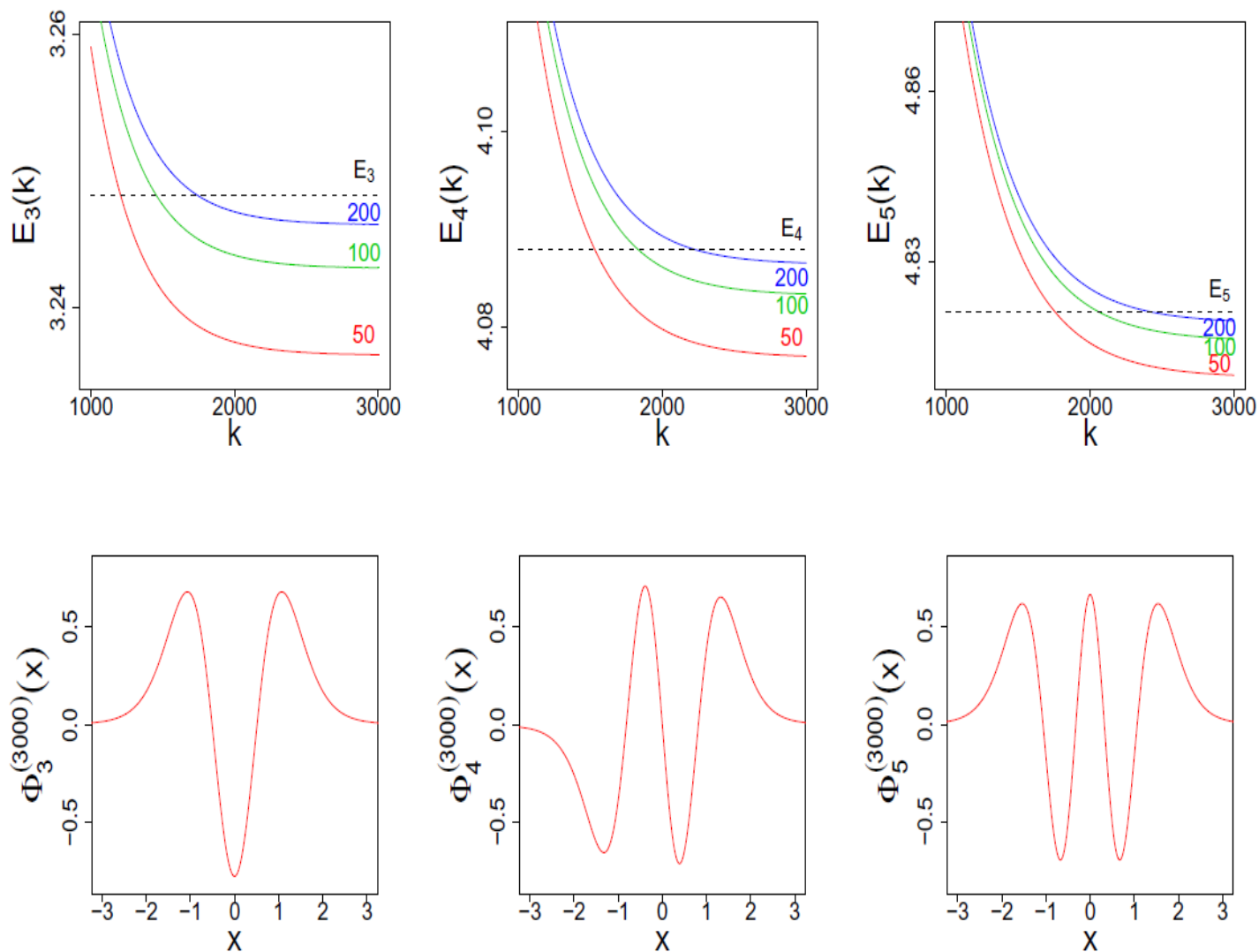


FIG. 6: The  $k$ -evolution of  $E_i^{(k)}$  for  $i = 3, 4, 5$  in the computation with  $0 \leq i \leq 4$  Hermite trial functions. The dependence on  $a$  is displayed as well. The corresponding (both limiting and approximating) eigenfunctions, labeled by  $i = 3, 4, 5$ , are depicted for  $x \in [-3, 3]$ .  $a \geq 50$  is used in the course of algorithmic iterations.

$$H(a)f(x) \sim [(-\Delta)^{1/2} + V(x)] f(x) = \frac{1}{\pi} \int_{|z| \leq a} \frac{f(x) - f(x+z)}{z^2} dz + V(x)f(x) \sim E(a) f(x)$$

$a = 50$ , instead of the previously mentioned  $[-3, 3]$ .

Let  $g(x)$  be another approximate spectral solution corresponding to the eigenvalue  $E(b)$ , with  $b > a$ , that is close to  $E(a)$  (as a member of a sequence converging to the limiting/genuine eigenvalue  $E$  associated with an eigenfunction  $\psi(x)$ ).

By our  $f \sim g$  assumption, a continuation of  $f$  from  $[-a, a]$  to  $[-b, b]$  does not differ considerably from  $g$  well beyond the control interval  $[-3, 3]$  (c.f. Figs. 1, 3, 6). We additionally assume the same about  $V(x)g(x)$  (for  $V(x) \sim x^2$  this would need  $g(x) \ll 1/x^2$ , in consistency with the estimate (11)). Therefore for  $x \in [-b, b]$  we have (keeping in mind that we evaluate the Cauchy principal value of the integral):

$$H(b)g(x) \sim \frac{1}{\pi} \int_{|z| \leq b} \frac{g(x) - g(x+z)}{z^2} dz + V(x)g(x) \sim E(a) g(x) + \frac{1}{\pi} \int_{a \leq |z| \leq b} \frac{g(x) - g(x+z)}{z^2} dz \sim \quad (13)$$

$$E(a) g(x) + \frac{2}{\pi} g(x) \int_a^b \frac{dz}{z^2} \sim \left[ E(a) + \frac{2}{\pi} \left( \frac{1}{a} - \frac{1}{b} \right) \right] g(x) \sim E(b)g(x)$$

Hence

$$E(b) - E(a) \sim \frac{2}{\pi} \left( \frac{1}{a} - \frac{1}{b} \right). \quad (14)$$

Inserting consecutive boundary values 50, 100, 200, 500 in the above formula we arrive at a perfect agreement with the numerically retrieved  $E(b) - E(a)$  data. Namely, we have:  $(2/\pi)(1/50 - 1/100) \sim 0.0064$ ,  $(2/\pi)(1/100 - 1/200) \sim 0.0032$ ,  $(2/\pi)(1/200 - 1/500) \sim 0.0019$  and ultimately  $(2/\pi)(1/500 - 1/\infty) \sim 0.0013$ .

Cauchy oscillator: **validity threshold** for the approximate eigenvalue formula

$$E_n^{appr} = \left(\frac{3\pi}{8}\right)^{2/3} [8n + (-1)^n]^{2/3}$$

$$\begin{aligned} E_2^{exact} &= 2.3381, & E_2^{appr} &= 2.32025, \\ E_4^{exact} &= 4.0879, & E_4^{appr} &= 4.08181, \\ E_6^{exact} &= 5.5206, & E_6^{appr} &= 5.51716, \\ E_8^{exact} &= 6.7867, & E_8^{appr} &= 6.78445, \\ E_{10}^{exact} &= 7.9440, & E_{10}^{appr} &= 7.94248, \\ E_{12}^{exact} &= 9.0226, & E_{12}^{appr} &= 9.02137, \\ E_{14}^{exact} &= 10.0402, & E_{14}^{appr} &= 10.03914, \\ E_{16}^{exact} &= 11.0085, & E_{16}^{appr} &= 11.00776, \\ E_{18}^{exact} &= 11.9360, & E_{18}^{appr} &= 11.93532. \end{aligned}$$

$$\begin{aligned} E_1^{exact} &= 1.0188, & E_1^{appr} &= 1.11546, \\ E_3^{exact} &= 3.2482, & E_3^{appr} &= 3.26163, \\ E_5^{exact} &= 4.8201, & E_5^{appr} &= 4.82632, \\ E_7^{exact} &= 6.1633, & E_7^{appr} &= 6.16712, \\ E_9^{exact} &= 7.3721, & E_9^{appr} &= 7.37485, \\ E_{11}^{exact} &= 8.4884, & E_{11}^{appr} &= 8.49050, \\ E_{13}^{exact} &= 9.5354, & E_{13}^{appr} &= 9.53705, \\ E_{15}^{exact} &= 10.5276, & E_{15}^{appr} &= 10.52897, \\ E_{17}^{exact} &= 11.4751, & E_{17}^{appr} &= 11.4762, \\ E_{19}^{exact} &= 12.3848, & E_{19}^{appr} &= 12.3857. \end{aligned}$$

The approximation accuracy threshold depends on the accepted robustness level. We are inclined to accept **n=10**. Note that „exact” values are known to be reproducible up to 14 or more decimal digits ! Here 50 digits:

Ex: Airy first zero **-2.3381**1074104597670384891972524467354406385401456724

**Cauchy finite well** eigenvalue problem:  
trigonometric connections ? Not quite ...

$$V(x) = \begin{cases} 0, & |x| < 1; \\ V_0, & |x| \geq 1. \end{cases}$$

$$\Phi_{n=2m+1}^{(0)}(x) = \begin{cases} A \cos\left(\frac{n\pi x}{2}\right), & |x| < 1, \\ 0, & |x| \geq 1 \end{cases} \quad \Phi_{n=2m}^{(0)}(x) = \begin{cases} A \sin\left(\frac{n\pi x}{2}\right), & |x| < 1, \\ 0, & |x| \geq 1 \end{cases} \quad m = 0, 1, \dots$$

A equals  $\pm 1$

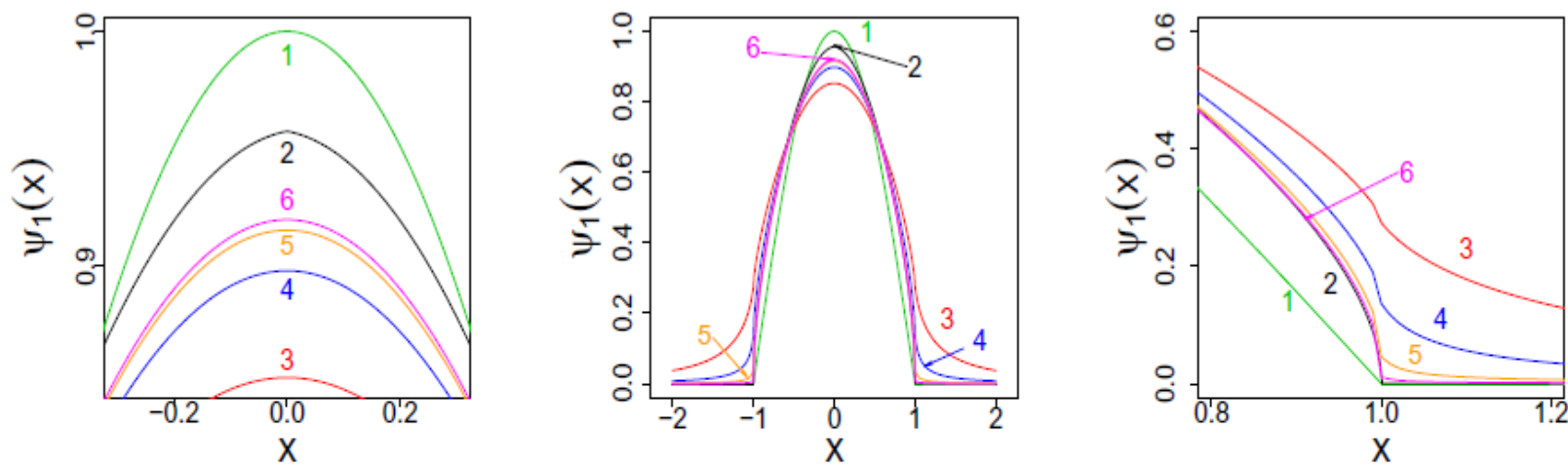


FIG. 7: Ground state solution of the Cauchy well. Numbers refer to: 1 -  $\cos(\pi x/2)$ , 2 - an approximate solution, Eq. (13) in [16], 3,4,5,6 refer to the well depths, respectively 5, 20, 100, 500. Convergence symptoms (towards an infinite well solution) are visually identifiable. Left panel reproduces an enlarged resolution around the maximum of the ground state. The right panel does the same job in the vicinity of the right boundary  $+1$  of the well (curves deformation comes from scales used to increase a resolution).

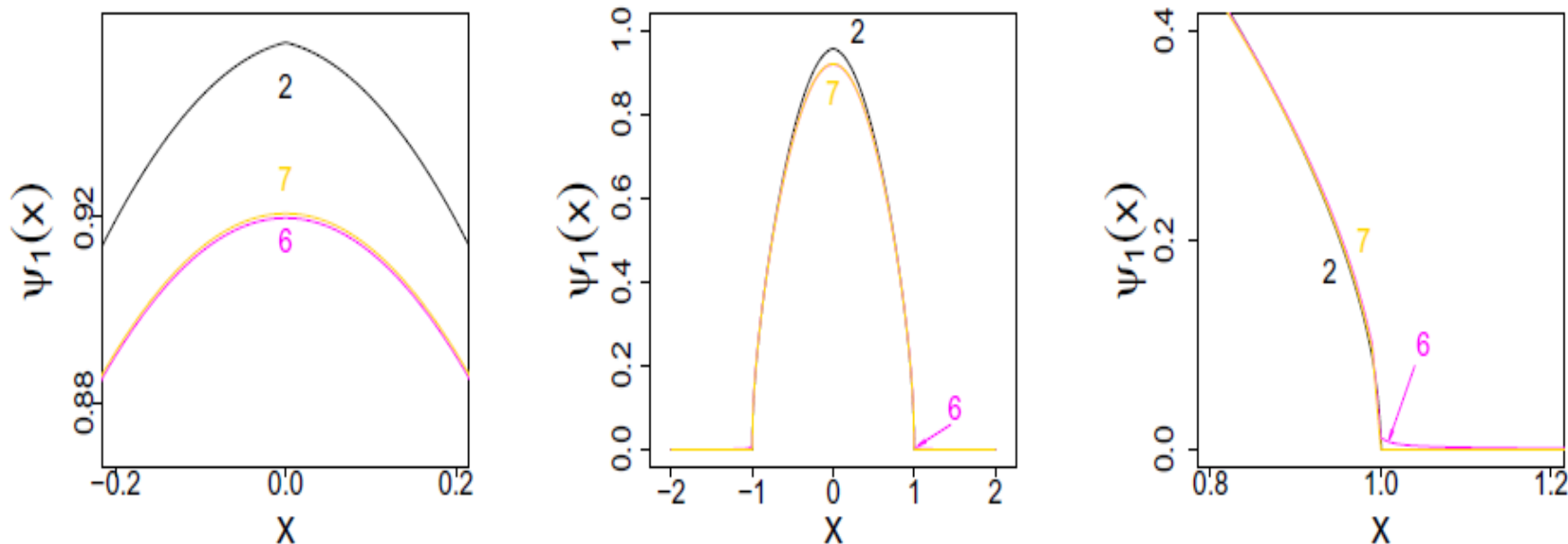


FIG. 8: Convergence towards  $\psi_1: 2$  - an approximate ground state, Eq. (13) in [16]; Our algorithm appears to be more reliable, since 6 and 7 refer to wells whose depths are respectively 500 and 5000. Left panel shows an enlarged vicinity of the maxima. Right panel shows enlarged plots in the vicinity of  $+1$ .

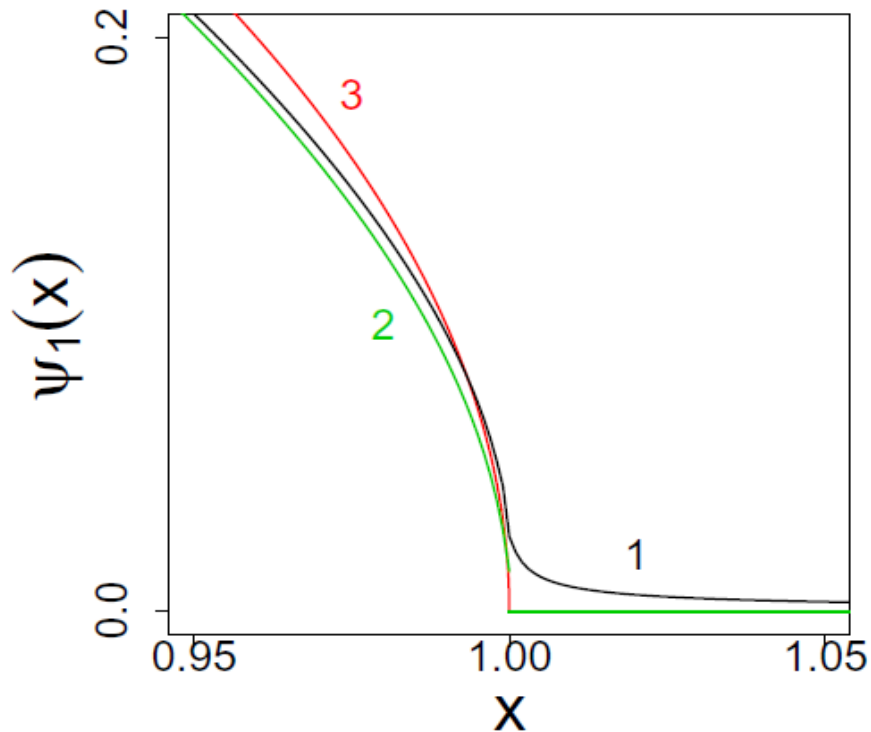


FIG. 9: Finite versus infinite Cauchy well ground state in the vicinity of the boundary +1 of  $[-1, 1]$ : 1 (black) - the algorithm outcome for the finite  $V_0 = 500$  well, 2 (green) - an approximate infinite well expression from Ref. [16], 3 (red) - an approximate form of  $\psi_1(x) \sim (1 - |x|)^{1/2}$ , in the vicinity of the infinite well barriers, as proposed in Ref. [11].

$a \backslash V_0$	5	20	100	500	5000
50	0.9538	1.0743	1.1258	1.1408	1.1445
100	0.9602	1.0807	1.1322	1.1472	1.1509
200	0.9634	1.0839	1.1353	1.1504	1.1541
500	0.9653	1.0858	1.1372	1.1523	1.1560

Approximate ground state eigenvalue for various well depths  $V_0$  and integration volume bounds  $a$ .

$E(200) - E(100) \sim 0.0032$ ,  $E(500) - E(200) \sim 0.0019$ .

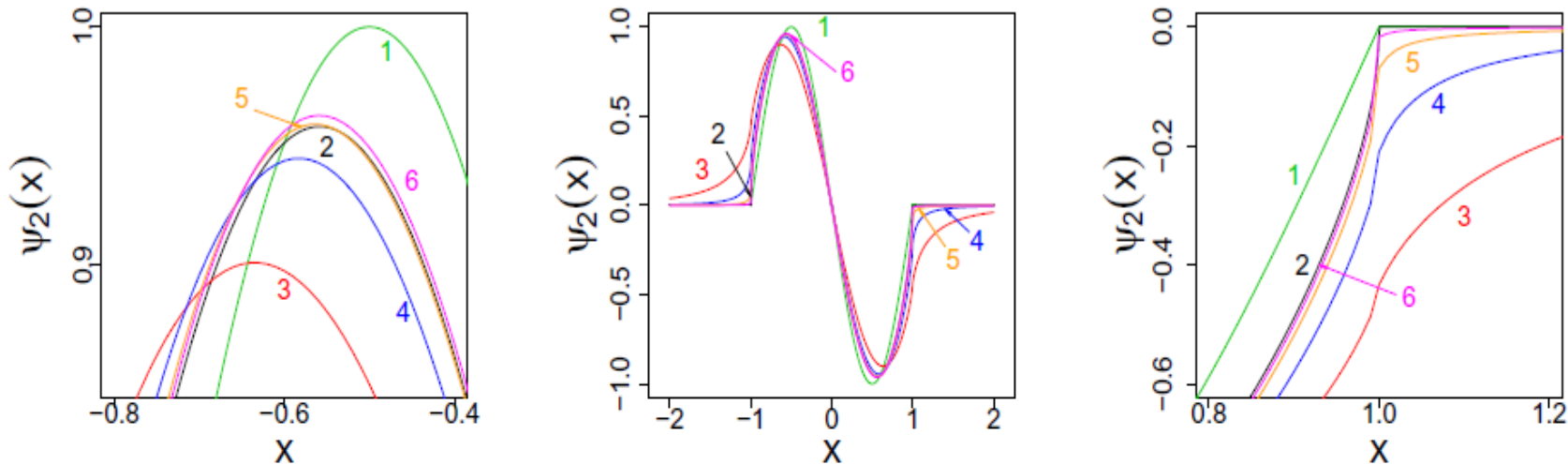


FIG. 10: First excited state  $\psi_2$ . Numbers refer to: 1 -  $-\sin(\pi x)$ , 2 - an approximate solution (13) of Ref. [16], 3, 4, 5, 6 correspond to finite wells with depths  $V_0 = 5, 20, 100, 500$  respectively. In the left panel we display an enlarged vicinity of the maximum of  $\psi_2$ . The right panel contains an enlargement of closely packed curves in the vicinity of the right boundary 1 of the well. Note the scales employed.

$a \backslash V_0$	5	20	100	500	5000
50	2.3701	2.6060	2.7046	2.7343	2.7419
100	2.3765	2.6124	2.7110	2.7407	2.7483
200	2.3797	2.6156	2.7142	2.7439	2.7515
500	2.3816	2.6175	2.7161	2.7458	2.7534



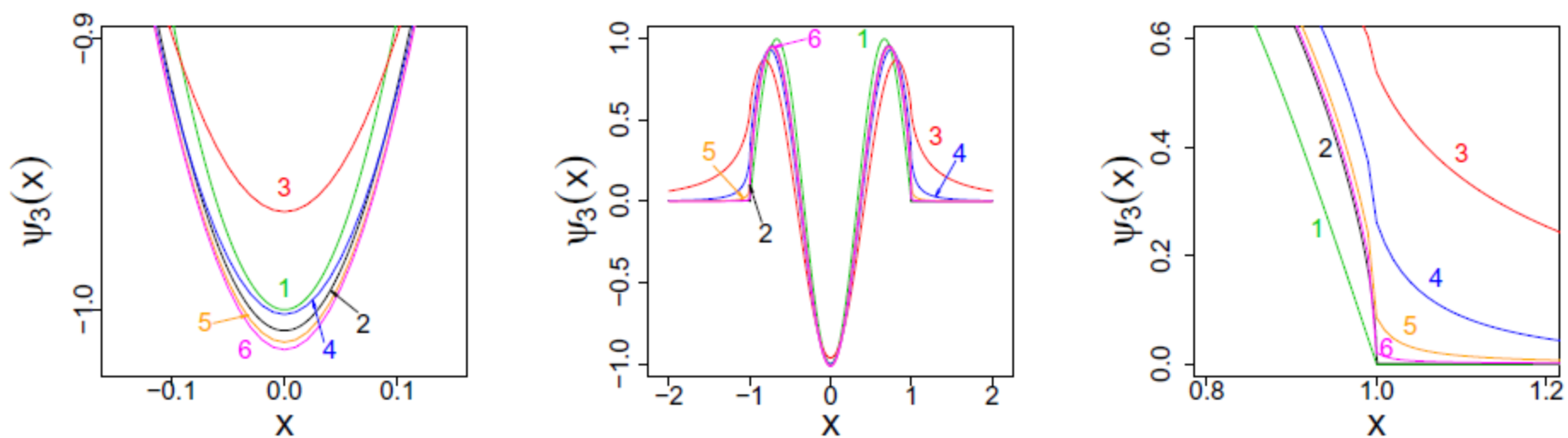
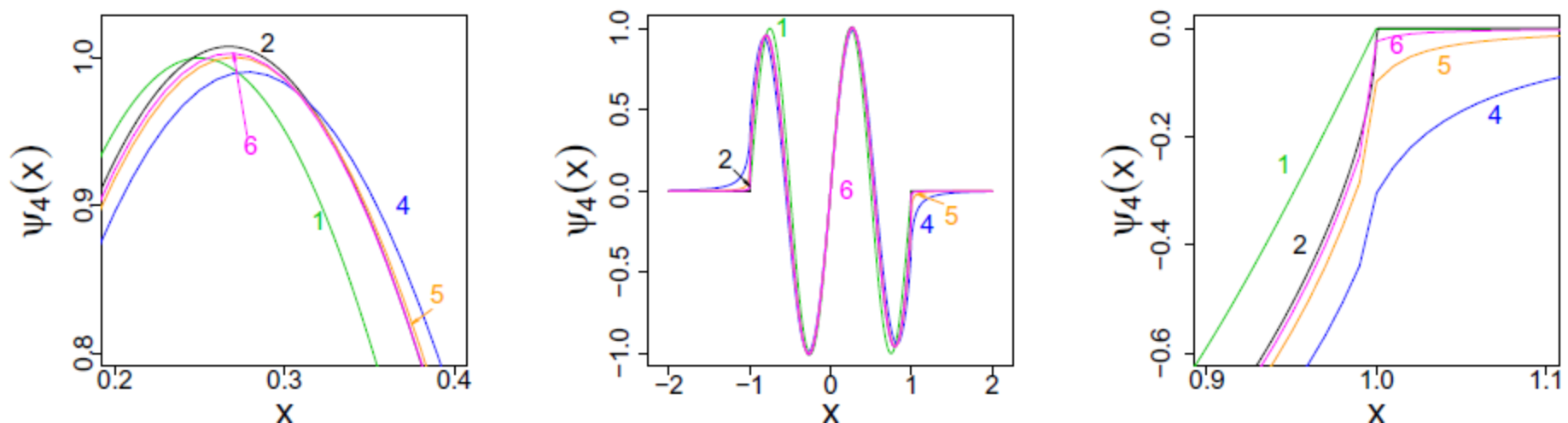


FIG. 11: Eigenstate  $\psi_3$ . Numbers refer to: 1 -  $-\cos(3\pi x/2)$ , 2 - approximate solution (13) of Ref. [16], 3, 4, 5, 6 correspond to well depths  $V_0 = 5, 20, 100, 500$ . Left panel contains an enlargement of a minimum of  $\psi_3$ . Right panel depicts an enlargement of closely packed curves in the vicinity of the well boundary.

0



# Quasirelativistic harmonic oscillator

$$H = T_m + V = [\sqrt{-\Delta + m^2} - m] + x^2$$

trial functions

$$\Phi_{n=2l-1}^{(0)}(x) = \begin{cases} A \cos\left(\frac{n\pi x}{2}\right), & |x| < 1, \\ 0, & |x| \geq 1 \end{cases} \quad \Phi_{n=2l}^{(0)}(x) = \begin{cases} A \sin\left(\frac{n\pi x}{2}\right), & |x| < 1, \\ 0, & |x| \geq 1 \end{cases} \quad l = 1, 2, \dots$$

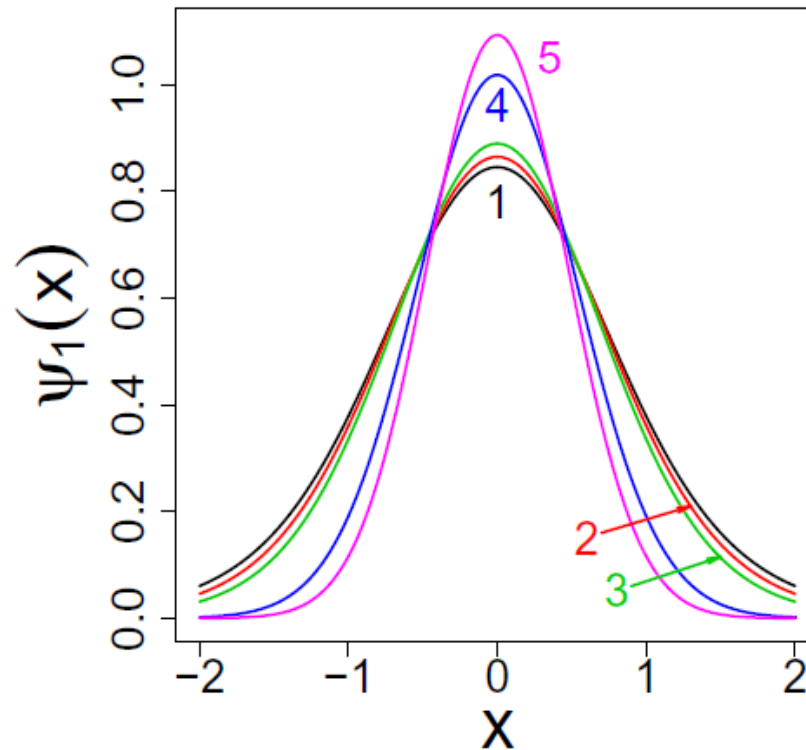
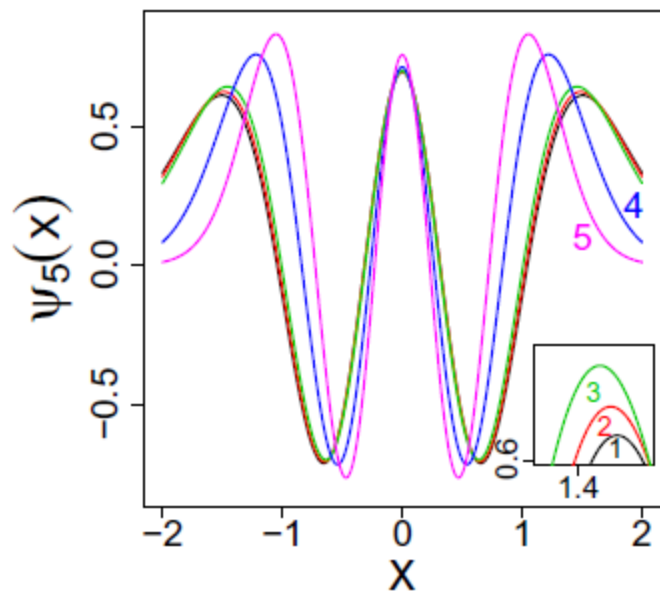
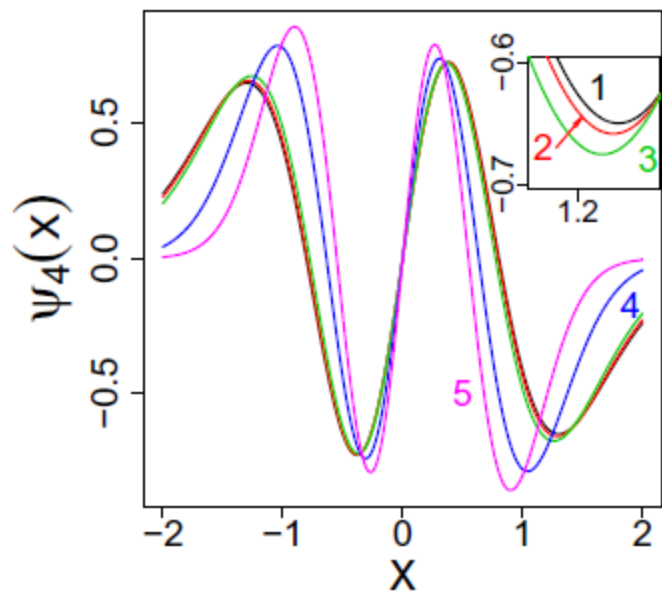
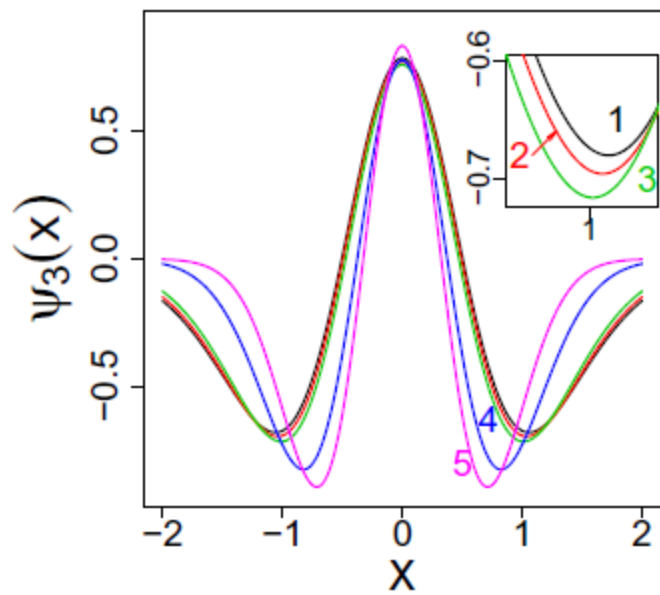
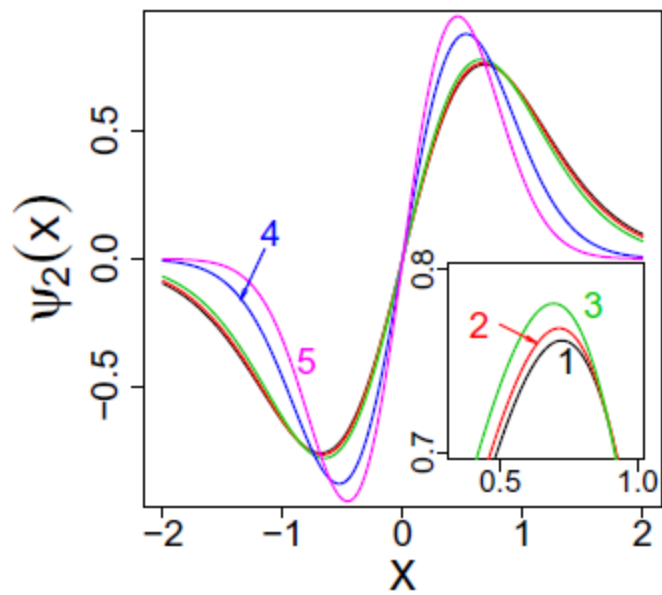


FIG. 1: Quasirelativistic oscillator ground state ( $n=1$ ) is depicted for masses  $m = 0.01, 0.5, 1, 5, 10$ , labeled respectively by 1, 2, 3, 4, 5. A clear distinction is seen between tentative "small" mass  $m \leq 1$  and "large" mass  $m \geq 5$  regimes. The  $m = 0.01$  curve is *fapp* identical with the ground state of the Cauchy oscillator, whose decay is known to be inverse polynomial  $\sim C/x^4$ , [2, 4].



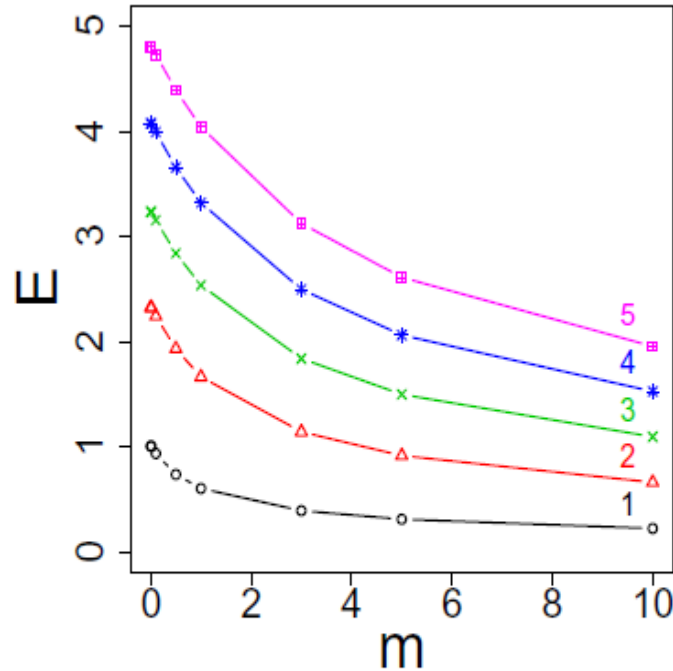


FIG. 3: The  $m$  dependence of the quasirelativistic oscillator eigenvalues with  $n = 1, 2, 3, 4, 5$ . Employed  $m > 0$  values read: 0.001, 0.01, 0.1, 0.5, 1, 3, 5, 10. The  $m = 0$  energy values have been directly imported from the spectral solution of the Cauchy oscillator [4, 5] and cannot be graphically distinguished from those for  $m = 0.001$ .

$V(x) = x^2$	$m=1$	$m = 3$	$m = 5$	$m = 10$	$m = 20$	$m = 50$	$m = 100$
$E_1$	0.6020	0.39043	0.30891	0.22112	0.15669	0.09936	0.06865
$E_2$	1.6638	1.1408	0.91436	0.65998	0.46904	0.29639	0.20562
$E_3$	2.5362	1.8385	1.4974	1.0939	0.77957	0.49125	0.34230
$E_4$	3.3210	2.4971	2.0620	1.5252	1.0886	0.68591	0.47874
$E_5$	4.0426	3.1253	2.6111	1.9540	1.3962	0.88136	0.61508

TABLE I: Quasirelativistic oscillator:  $m$ -dependence of lowest five eigenvalues.

$m \ll 1$  regime

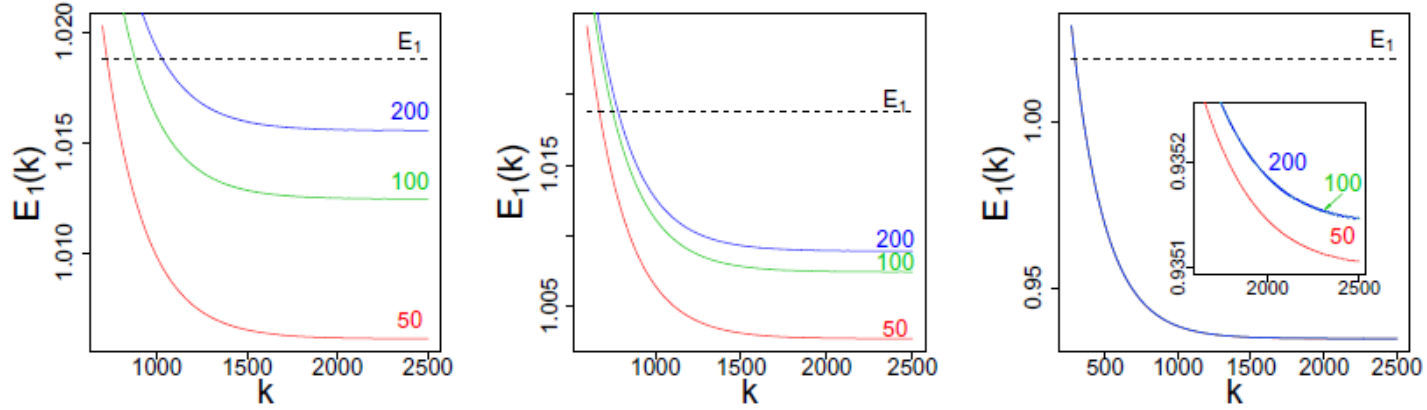


FIG. 4:  $(k)$ -time evolution of  $E_1^{(k)}(h) = -\frac{1}{h} \ln(\mathcal{E}_1^k(h))$  (8) and the stabilization symptoms in the computation of the ground state value:  $m = 0.001$  (left panel),  $m = 0.01$  (middle panel) and  $m = 0.1$  (right panel), for  $a = 50, 100, 200$ . For reference we have depicted the energy level  $E_1 = 1.018792$  which is set by the Cauchy oscillator bottom eigenvalue.

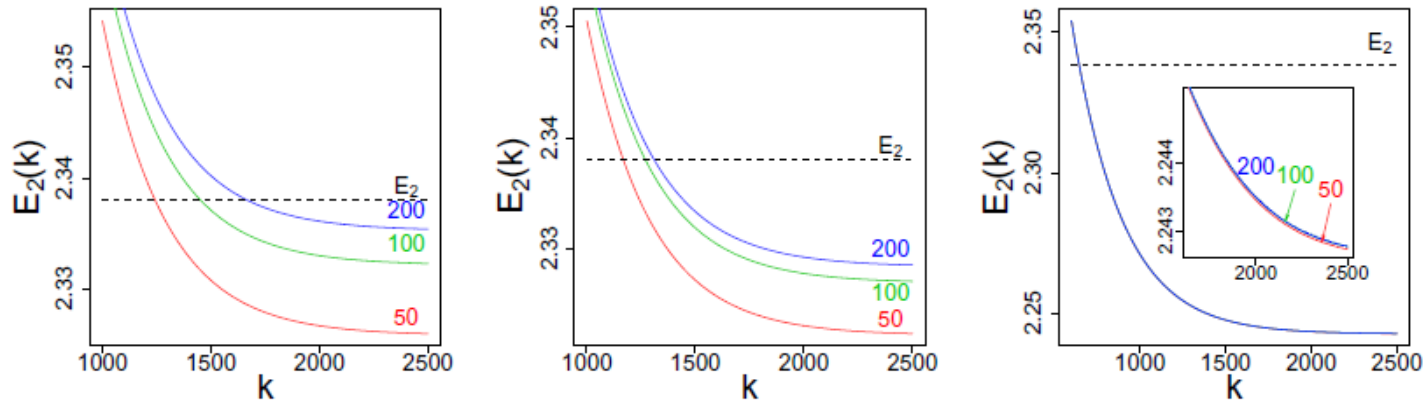


FIG. 5:  $(k)$ -time evolution of  $E_2^{(k)}(h) = -\frac{1}{h} \ln(\mathcal{E}_2^k(h))$  (8). Computation of the first excited eigenvalue for  $m = 0.001$  (left panel),  $m = 0.01$  (middle panel),  $m = 0.1$  (right panel), for  $a = 50, 100, 200$ .  $E_2 = 2.338107$  is the first excited Cauchy oscillator eigenvalue.

*Spectral convergence to the Cauchy oscillator.*

m=0	$E_1$	$E_2$	$E_3$	$E_4$	$E_5$
[4, 5]	1.018792	2.338107	3.248197	4.087949	4.820099

TABLE II: Cauchy oscillator lowest eigenvalues.

m=0.001	$E_1$	$E_2$	$E_3$	$E_4$	$E_5$
a=50	1.00612	2.32596	3.23723	4.07956	4.81614
a=100	1.01245	2.33229	3.24356	4.08590	4.82248
a=200	1.01555	2.33540	3.24667	4.08901	4.82560

TABLE III: Quasirelativistic oscillator:  $a$ -dependence of lowest eigenvalues for  $m = 0.001$ .

m=0.01	$E_1$	$E_2$	$E_3$	$E_4$	$E_5$
a=50	1.00275	2.32235	3.23367	4.07593	4.81255
a=100	1.00746	2.32707	3.23839	4.08066	4.81728
a=200	1.00893	2.32854	3.23987	4.08213	4.81876

$$E_{n=2k-1} \sim \left(\frac{3\pi}{2}\right)^{2/3} \left(n + \frac{3}{4}\right)^{2/3} \quad 1.$$

$$E_{n=2k} \sim \left(\frac{3\pi}{2}\right)^{2/3} \left(n + \frac{1}{4}\right)^{2/3}$$

$m \gg 1$  regime

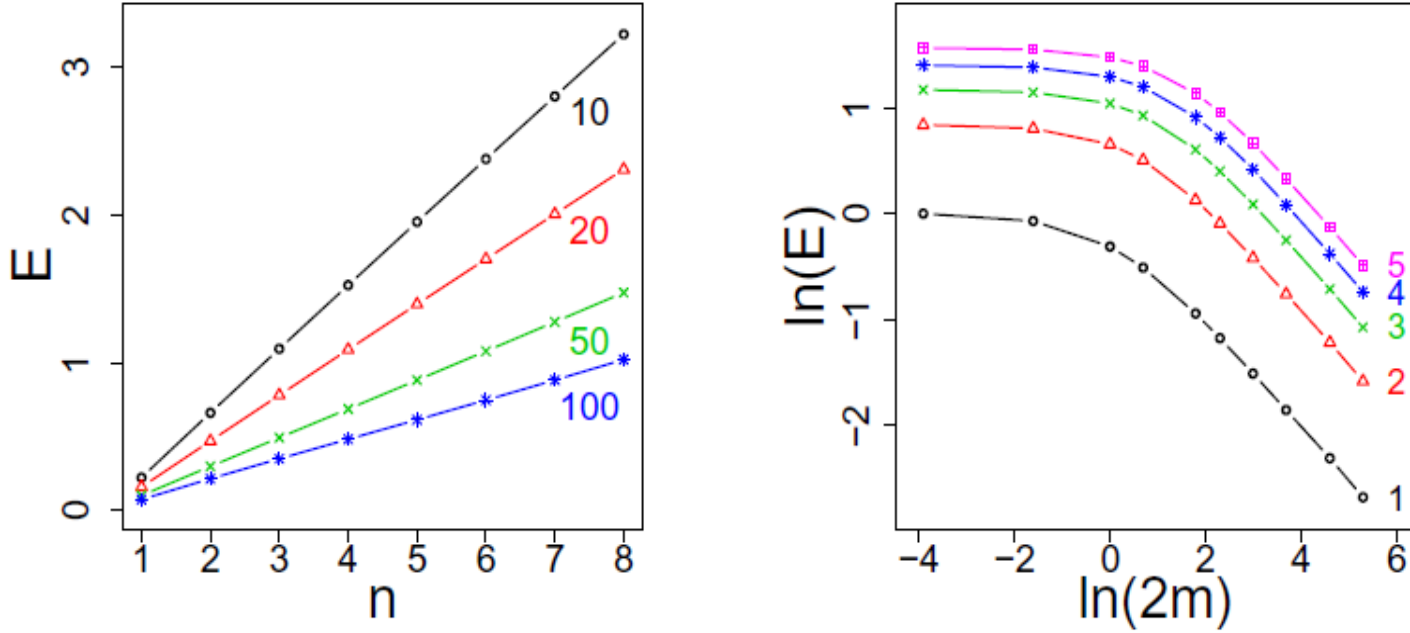


FIG. 6: Quasirelativistic  $m \gg 1$  regime. Left panel: eight consecutive eigenvalues  $E_n(m)$ , for masses  $m = 10, 20, 50, 100$ , build an approximate a straight line  $E_n(m) = \frac{1}{\sqrt{2m}}(2n - 1)$ ,  $n \geq 1$ . The best result is obtained if fitting employs  $m \geq 10$ . Right panel: doubly logarithmic scale gives access to a wider mass range:  $m = 0.01, 0.1, 0.5, 1, 3, 5, 10, 20, 50, 100$ . Note that for  $m > 3.7$  i.e.  $\ln(2m) > 2$ , straight line segments are mimicked by  $\ln(E_n(m)) = -\frac{1}{2} \ln(2m) + \ln(2n - 1)$ ,  $n = 1, 2, 3, 4, 5$ , thus reproducing the nonrelativistic oscillator spectral pattern.

$$E_n(m) = \frac{1}{\sqrt{2m}}(2n - 1), \quad n = 1, 2, \dots \quad m \gg 1,$$

$$\ln[E_n(m)] = -\frac{1}{2} \ln(2m) + \ln(2n - 1), \quad n = 1, 2, \dots \quad m \gg 1$$

# Quasirelativistic finite well

$$V(x) = \begin{cases} 0, & |x| < 1 \\ V_0, & |x| \geq 1 \end{cases}$$

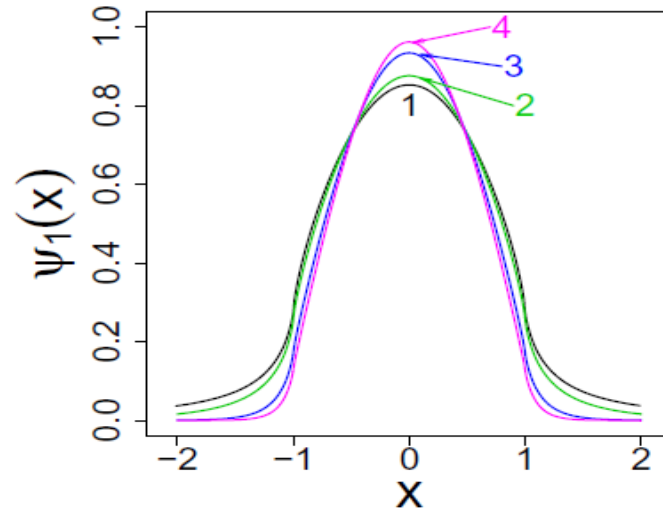


FIG. 7: Quasirelativistic finite well ground state for  $V_0 = 5$ . Labels 1, 2, 3, 4 correspond to  $m = 0.01, 1, 5, 10$ , respectively.

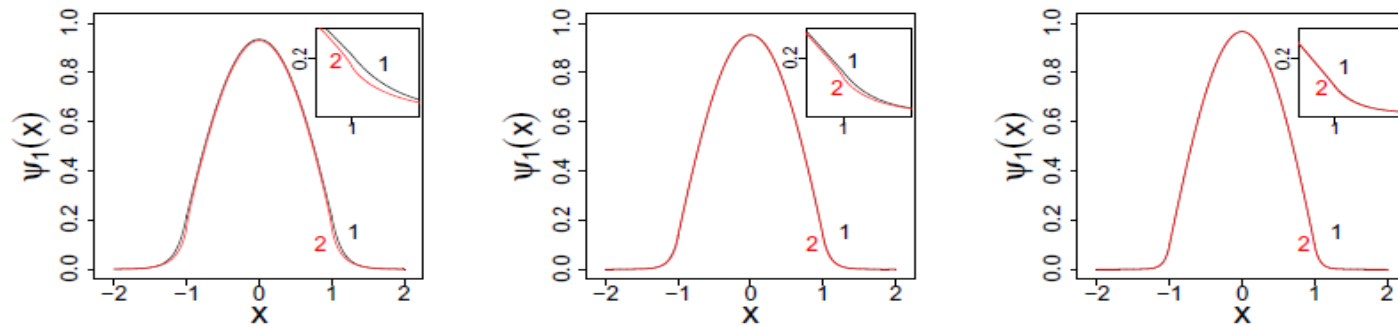


FIG. 8: A comparison of ground states in case of  $V_0 = 5$  for the nonrelativistic (label 1) and quasirelativistic well (label 2):  $m = 5$  (left panel),  $m = 10$  (middle panel),  $m = 20$  (right panel).



Shallow well.

mass	quasirelativistic $N$	standard $N$
0.1	3	1
0.5	4	2
1	4	3
3	5	4
5	6	5
10	7	7

$V_0 = 5$  well: maximal number  $N$  of bound states for various masses in quasirelativistic and nonrelativistic cases.

$$\frac{\pi^2}{8V_0}(N-1)^2 \leq m \leq \frac{\pi^2}{8V_0}N^2 \quad [-1, 1] \text{ choice}$$

mass	finite well	n=1	n=2	n=3	n=4	n=5	n=6	n=7	n=8
m=10	quasi	0.09951	0.39217	0.86271	1.48933	2.24605	3.10483	4.03221	-
	standard	0.10190	0.40679	0.91211	1.61267	2.49846	3.54752	4.68404	-
m=20	quasi	0.05312	0.21154	0.47264	0.83227	1.28482	1.82341	2.43999	3.12481
	standard	0.05379	0.21502	0.48318	0.85739	1.33616	1.91714	2.59636	3.36634
m=50	quasi	0.02227	0.08892	0.19968	0.35423	0.55213	0.79272	1.07522	1.39867
	standard	0.02261	0.09040	0.20334	0.36132	0.56421	0.81181	1.10385	1.43998
m=100	quasi	0.01126	0.04499	0.10113	0.17961	0.28037	0.40334	0.54842	0.71546
	standard	0.01159	0.04636	0.10431	0.18540	0.28964	0.41695	0.56733	0.74070

TABLE VII: Quasirelativistic (quasi) versus nonrelativistic (standard)  $V_0 = 5$  well:  $m$ -dependence of eigenvalues

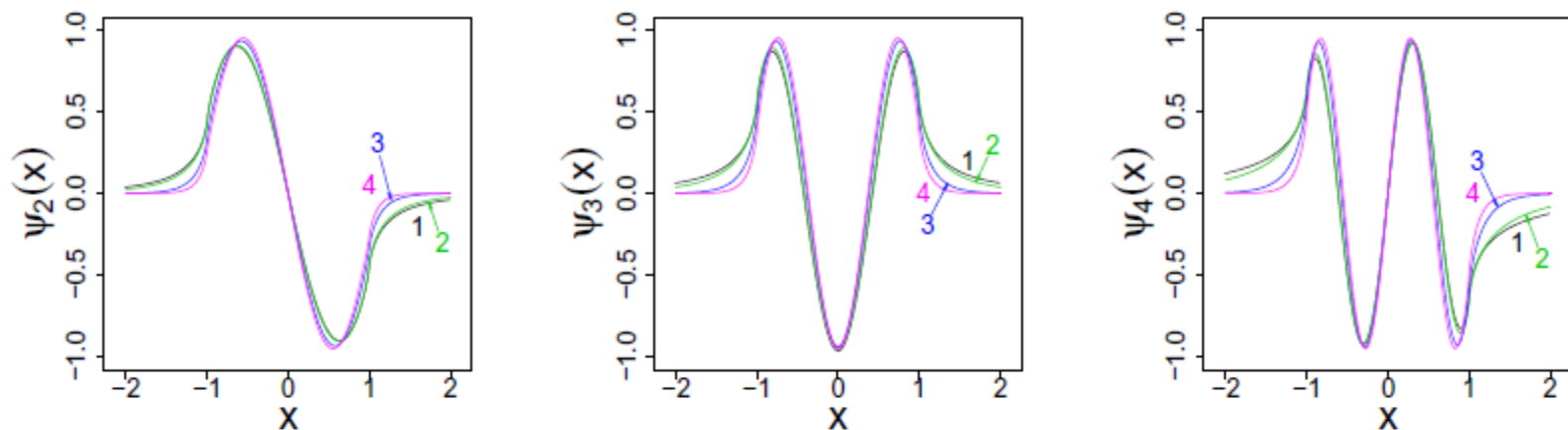


FIG. 9: Second, third and fourth quasirelativistic  $V_0 = 5$  well eigenfunctions. Masses  $m = 0.01, 1, 5, 10$  are labeled respectively by 1, 2, 3, 4.

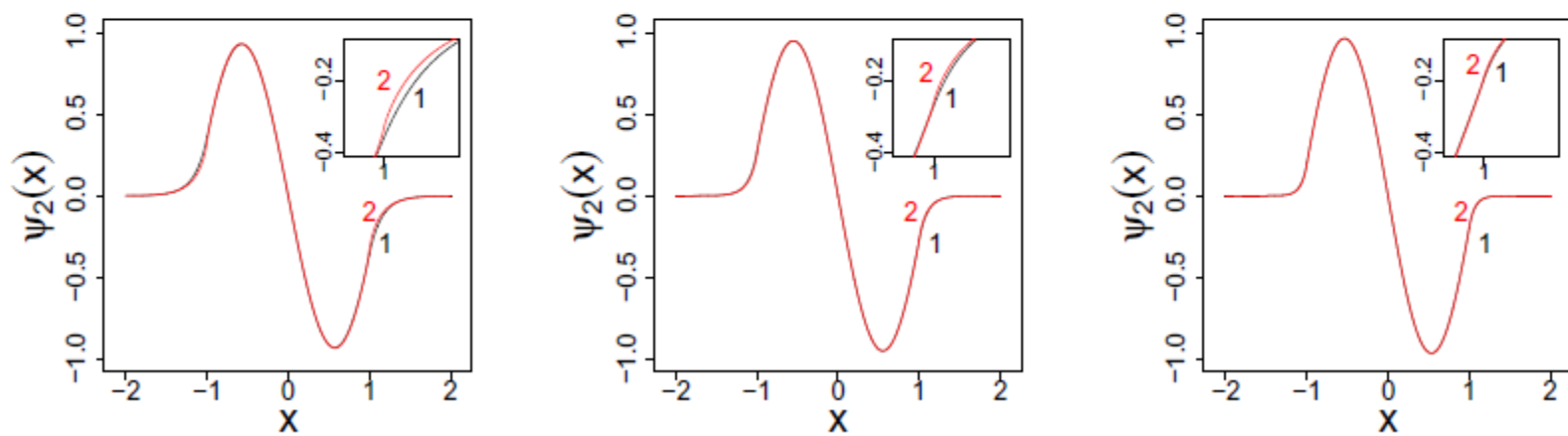


FIG. 10: A comparison of the second eigenfunction in the  $V_0 = 5$  well for nonrelativistic (label 1) and quasirelativistic (label 2) cases. Here,  $m = 5$  (left panel),  $m = 10$  (middle panel),  $m = 20$  (right panel).

Deep well versus infinite well.  $E_n - mc^2 = \left(\frac{n\pi}{2} - \frac{\pi}{8}\right) \frac{\hbar c}{b} + O\left(\frac{1}{n}\right)$   $[-b, b]$  infinite Cauchy ( $m = 0$ ) well

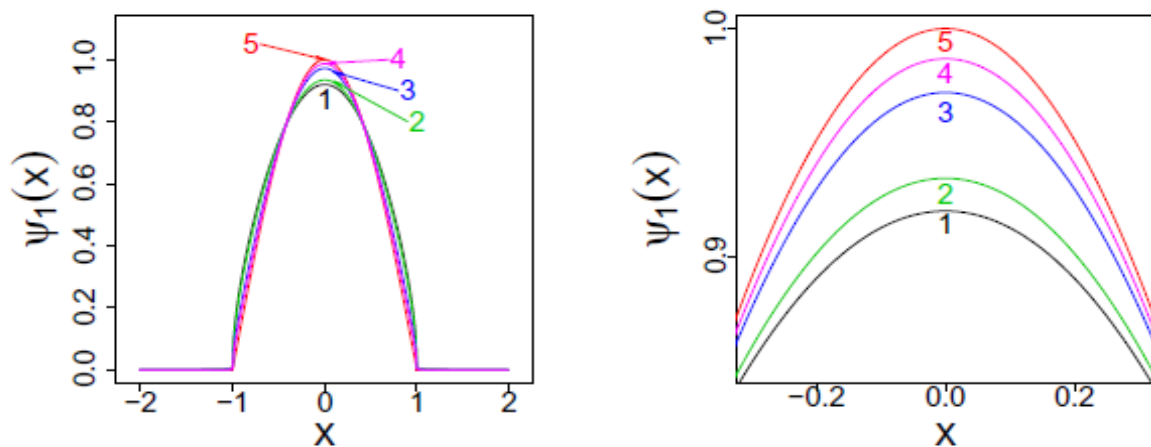


FIG. 12: Quasirelativistic  $V_0 = 500$  ground state. Labels 1, 2, 3, 4 refer to masses  $m = 0.01, 1, 5, 10$ . Label 5 refers to the nonrelativistic infinite well ground state  $\cos(\pi x/2)$ . Right panel: an enlargement of the vicinity of the maximum.

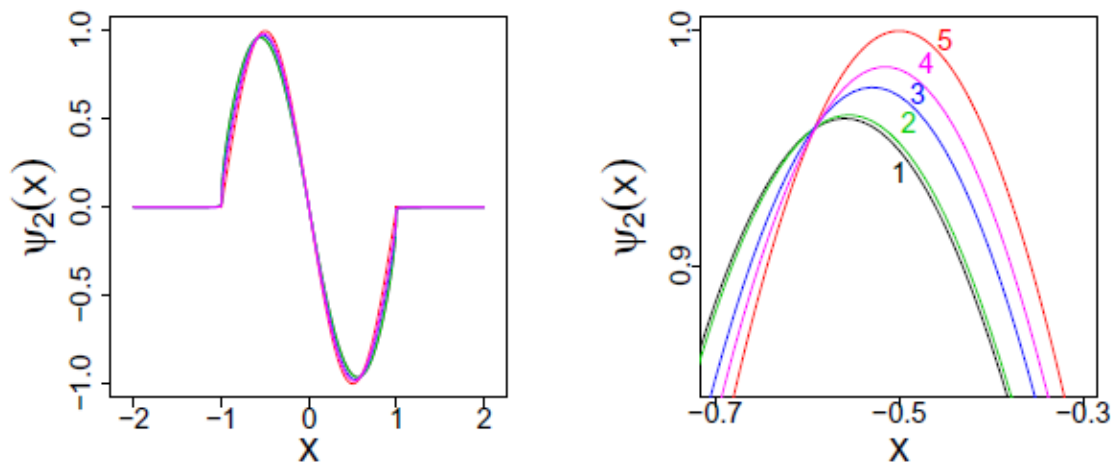


FIG. 13: First excited state of the  $V_0 = 500$  well. Labels 1, 2, 3, 4 refer to  $m = 0.01, 1, 5, 10$ , label 5 to the curve  $-\sin(\pi x)$ . Right panel: enlargement of the vicinity of maximum.

# Spectral affinities: Cauchy well versus nonrelativistic well (finite but deep !)

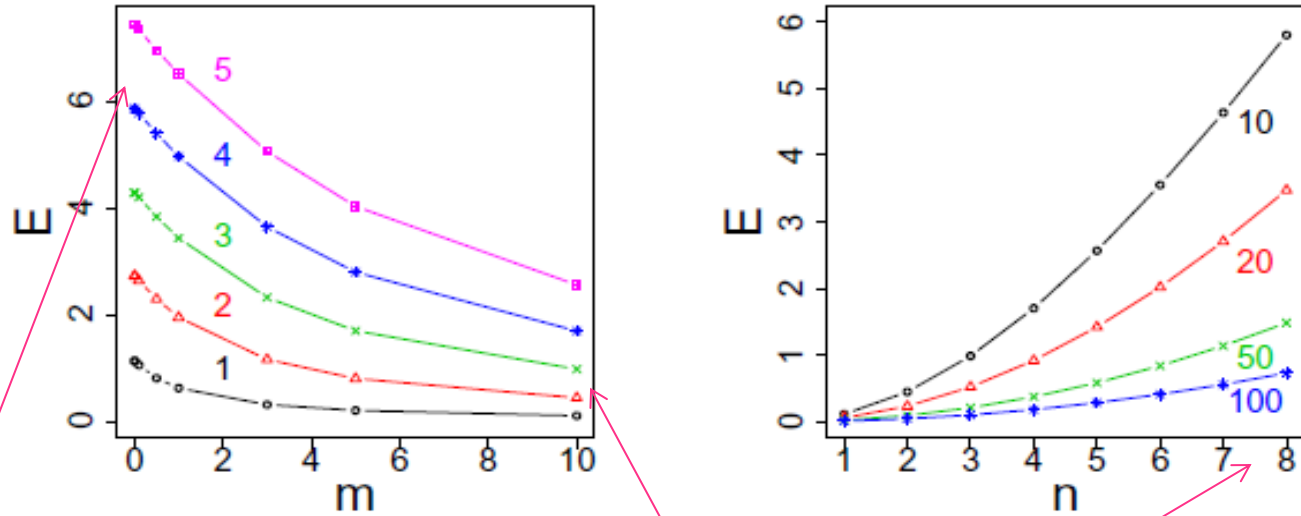



FIG. 16:  $V_0 = 500$  quasirelativistic well. Left panel:  $E_n$  dependence on  $m$ ,  $n = 1, 2, 3, 4, 5$ . Right panel: computed eigenvalues are depicted against  $n = 1, 2, 3, 4, 5$ . For each mass value ( $m = 10, 20, 50, 100$ ) we depict a curve which is an optimal fit to the data.

$$E_n - mc^2 = \left(\frac{n\pi}{2} - \frac{\pi}{8}\right) \frac{\hbar c}{b} + O\left(\frac{1}{n}\right)$$

$[-b, b]$

$$E_n^{V_0} \approx E_n^\infty \left(1 - \frac{4}{\pi\sqrt{V_0}}\right) = \frac{\pi^2 n^2}{8m} \left(1 - \frac{4}{\pi\sqrt{V_0}}\right)$$

$$\frac{4}{\pi\sqrt{V_0}} < 0.06 \text{ for } V_0 = 500.$$



n		m=0.01	m=0.1	m=0.5	m=1	m=3	m=5	m=10	m=20	m=50	m=100
1	nonrelat. deep	1.2160	1.2287	1.3677	1.6698	3.3408	5.2254	10.1188	20.0611	50.0245	100.0122
	$\infty$ -quasi 1.13	1.5708	1.5740	1.6484	1.8621	3.3864	5.2409	10.1226	20.0616	50.0247	100.0123
2	nonrelat. deep	2.9055	2.9089	2.9417	3.0760	4.2393	5.8600	10.4680	20.2435	50.0979	100.0486
	$\infty$ quasi 1.13	3.1416	3.1432	3.1811	3.2969	4.3439	5.9050	10.4819	20.2452	50.0986	100.0493
3	nonrelat. deep	4.5596	4.5623	4.5746	4.6500	5.4697	6.8085	11.0283	20.5443	50.2200	100.1093
	$\infty$ quasi 1.13	4.7124	4.7134	4.7388	4.8173	5.5863	6.8707	11.0547	20.5477	50.2216	100.1110
4	nonrelat. deep	6.2290	6.2308	6.2298	6.2734	6.8743	7.9735	11.7730	20.9585	50.3905	100.1943
	$\infty$ quasi 1.13	6.2832	6.2840	6.3030	6.3623	6.9626	8.0298	11.8101	20.9637	50.3932	100.1972
5	nonrelat. deep	7.8344	7.8365	7.8331	7.8633	8.3321	9.2502	12.6725	21.4803	50.6090	100.3033
	$\infty$ quasi 1.13	7.8540	7.8546	7.8699	7.9174	8.4074	9.3105	12.7155	21.4869	50.6131	100.3080

We compare eigenvalues of the  $V_0 = 500$  quasirelativistic well computed by two different approximation methods. We use a nonrelativistic approximation formula for the finite but very deep well and set the computed values against the upper bound for the infinite quasirelativistic well, e.g. Eq. (1.13) imported from (Kaleta, Kwasnicki, Malecki; 2013)

**Proposition 1.1.** *For all  $n = 1, 2, \dots$ , we have*

$$mc^2 \sqrt{\left(\frac{(n-1)\pi}{2} \frac{\hbar}{mca}\right)^2 + 1} < E_n \leq mc^2 \sqrt{\left(\frac{n\pi}{2} \frac{\hbar}{mca}\right)^2 + 1}. \quad (1.13)$$

Set  $c = \hbar = 1$  and  $a=1$ . Nonrelativistic approximation reliable for  $m > 10$ :

$$E_n^{V_0} \approx E_n^\infty \left(1 - \frac{4}{\pi\sqrt{V_0}}\right) = \frac{\pi^2 n^2}{8m} \left(1 - \frac{4}{\pi\sqrt{V_0}}\right)$$

# Spectral affinity / spectral convergence: an analytic argument

$$H = T_m + V$$

$$(T_m + mc^2)\phi(x) = \sqrt{m^2c^4 - \hbar^2c^2 \frac{\partial^2}{\partial x^2}} \phi(x)$$

$$\begin{aligned} (T_m + mc^2)\phi(x) &= \frac{mc^2}{\sqrt{2\pi}} \int_{-\infty}^{\infty} \bar{\phi}(k) dk \sqrt{1 - \frac{\hbar^2}{m^2c^2} \frac{\partial^2}{\partial x^2}} e^{ikx} = \\ &= \frac{mc^2}{\sqrt{2\pi}} \int_{-\infty}^{\infty} \bar{\phi}(k) dk \left[ 1 - \frac{\hbar^2}{m^2c^2} \frac{1}{2} \frac{\partial^2}{\partial x^2} - \left( \frac{\hbar^2}{m^2c^2} \right)^2 \frac{1}{8} \frac{\partial^2}{\partial x^2} - \dots \right] e^{ikx} = \\ &= \frac{mc^2}{\sqrt{2\pi}} \int_{-\infty}^{\infty} \bar{\phi}(k) dk \sqrt{1 + \frac{p^2}{m^2c^2}} e^{ikx} = \frac{1}{\hbar\sqrt{2\pi}} \int_{-\infty}^{\infty} dp \sqrt{m^2c^4 + p^2c^2} e^{ipx/\hbar} \bar{\phi}(p). \end{aligned}$$

$$\hbar/mc = \lambda_C \text{ and } p = \hbar k$$

Taylor series with respect to  $p^2/m^2c^2 = k^2\lambda_C^2$

$$\frac{mc^2}{\sqrt{2\pi}} \int_{-\infty}^{\infty} \bar{\phi}(k) dk \sqrt{1 + k^2\lambda_C^2} e^{ikx} \sim \frac{mc^2}{\sqrt{2\pi}} \int_{-\infty}^{\infty} \bar{\phi}(k) dk [1 + (1/2)k^2\lambda_C^2] e^{ikx} = mc^2\phi(x) - \frac{\hbar^2}{2m}\Delta\phi(x)$$

$$k^2\lambda_C^2 \ll 1,$$

electron  $\lambda_C = 0.00386\text{\AA}$

neutrino we have  $\lambda_C^\nu = 233\lambda_C \sim 0.8994\text{\AA}$

$$m^2c^2/p^2 = (k^2\lambda_C^2)^{-1}.$$

$$\frac{mc^2}{\sqrt{2\pi}} \int_{-\infty}^{\infty} \bar{\phi}(k) dk \sqrt{1 + k^2\lambda_C^2} e^{ikx} = \frac{\hbar c}{\sqrt{2\pi}} \int_{-\infty}^{\infty} \bar{\phi}(k) dk |k| \sqrt{1 + (k^2\lambda_C^2)^{-1}} e^{ikx} \sim \hbar c |\nabla| \phi(x)$$

$$k^2\lambda_C^2 \gg 1,$$

(Non-exhaustive) **summary of points** that need non-amateur **math.**

- **Path-wise** description of a jump-type process with killing; how do they set down at the stationary (ground) state ?
- A complementary **path-wise** description of the process which equilibrates to the „ground state „ pdf (**trapping** in a finite well !)
- „Spectral affinity” / **convergence** with mathematical rigour:  $m$  to  $0$  limiting behavior,  $m$  to infinity limiting behavior
- Maximal number of bound states in the quasirelativistic and Cauchy **finite wells**, from 1D to 3D
- More refined (as much analytic as possible) **analysis of shapes** of eigenfunctions. More accurate **eigenvalue estimates**.
- More refined analysis of **nonlocality impact** upon the computation of eigenvalues
- Spectral problems **in 3D** (partial results only for Cauchy and quasi oscillators)

**Source papers: collaboration with M. Žaba and V. Stephanovich;  
2010-2014**

Physica **A 389**, 4419-4435, (2010), Levy flights in inhomogeneous environments, with V. S. (spectral solution for 1D Cauchy oscillator)

J. Math. Phys. **54**, 072103, (2013), Levy flights and nonlocal quantum dynamics, with V. S. (general framework, lots of Fourier-related discussion, Cauchy wave-packet dynamics)

arXiv:1403.5668, Solving fractional Schrödinger-type spectral problems: Cauchy oscillator and Cauchy well, with. M. Z.

arXiv:1405.4724, Nonlocally-induced (quasirelativistic) bound states: Harmonic confinement and the finite well, with M. Z.